Computer Simulation of Static and Dynamic Properties During Transient Sorption of Fluids in Mesoporous Materials

ARTICLE *in* THE JOURNAL OF PHYSICAL CHEMISTRY C · NOVEMBER 2009

Impact Factor: 4.77 · DOI: 10.1021/jp903717b

1 AUTHOR:

Harald Morgner
University of Leipzig
132 PUBLICATIONS **1,805** CITATIONS

Computer Simulation of Static and Dynamic Properties During Transient Sorption of Fluids in Mesoporous Materials

Harald Morgner*

Wilhelm Ostwald-Institute for Physical and Theoretical Chemistry, Faculty of Chemistry and Mineralogy, University Leipzig, Linnestreet 2, D-04103 Leipzig

Received: April 22, 2009; Revised Manuscript Received: October 23, 2009

The hysteresis observed frequently in the adsorption isotherm of gas in porous material is currently subject to intense research. The nature of the hysteresis itself and in particular recent observations on the uptake dynamics inside the hysteresis loop are described as poorly understood puzzles even in recent literature (Wallacher, D.; Künzer, N.; Kovalev, D.; Knorr, N.; Knorr, K. *Phys. Rev. Lett*. **2004**, *92*, 195704-1; Valiullin, R.; Naumov, S.; Galvosas, P.; Kärger, J.; Woo, H.-J.; Porcheron, F.; Monson, P. *Nature* **2006**, *443*, 965−968). Detailed experiments combined with theoretical efforts have led to the identification of new problems rather than answers, e.g., the relaxation dynamics in pressure jump experiments is found to be "dramatically" slowed down inside the hysteresis loop (Valiullin et al. 2006). This has motivated the authors to postulate "a fundamental difference in the nature of the relaxation dynamics for states within the hysteresis region compared with those outside of this region". Here we present a computer simulation study on cylindrical pores. We determine the adsorption isotherm, i.e., a steady state property, and the uptake dynamics inside and outside of the hysteresis loop. Further, we study the behavior during incomplete passage through the hysteresis loop, a situation which has been characterized recently by PFG NMR (pulsed field gradient nuclear magnetic resonance) and again has motivated elaborate explanations (Naumov et al. 2008). It is noteworthy that all experimental observations are reproduced when describing diffusion by the Onsager ansatz which employs the gradient of the chemical potential as driving force. No ad hoc assumptions about a new transport mechanism inside the hysteresis region are needed.

Introduction

The progress in synthesizing porous materials with a narrow distribution of pore diameters in the mesoporous range has raised the interest in exploring possible applications as well as in understanding the basic properties. An important phenomenon is the observation that the amount of an atomic or molecular species adsorbed from the gas phase not only is dependent on the gas pressure, but also may depend in certain ranges of pressure on the history. When raising the pressure, the adsorbed amount may be smaller than that observed while lowering the pressure. As the shape of the adsorption isotherm is reminiscent of the hysteresis in ferromagnetic materials, the term adsorption hysteresis is commonly used for this phenomenon. Even though it has been known for many decades, its explanation is still under intense investigation. The current status of the discussion explains the existence of the adsorption hysteresis by the involvement of metastable states[1] and, consequently, by "a failure of the system to equilibrate".[2] In order to get a handle on the behavior of adsorbed matter in porous materials, a group of authors has recently evaluated the self-diffusion coefficient by means of PFG NMR (pulsed field gradient nuclear magnetic resonance).[2] They found the self-diffusion coefficient to depend on the amount of pore filling as expected, but beyond that they noted a small, but significant, deviation between adsorption and desorption branches of the hysteresis loop for equal amounts of adsorbate. While the self-diffusion coefficient is measured for constant gas pressure and, thus, characterizes a stable situation, the transport of matter within the porous material has been assessed by pressure jump experiments leading to the evaluation of a relaxation time. Wallacher et al.[1] have manufactured mesoporous silicon with regularly etched noninterconnected pores. They found for adsorption of nitrogen at 77.2 K that the characteristic relaxation time within the hysteresis loop deviates by orders of magnitude from the relaxation time outside the hysteresis loop.[1] This observation has been confirmed for adsorption of cyclohexane in Vycor porous glass.[2] In summary, we state that in the literature several key points with respect to adsorption hysteresis are discussed: the relaxation time during pressure jump experiments,[1,2] the behavior of the self-diffusion coefficient within the hysteresis loop after long times,[2] the behavior of the self-diffusion coefficient during incomplete passage (scanning curves) through the hysteresis loop,[3] the existence of the hysteresis. The assumed involvement of metastable states makes even the observed reproducibility of the hysteresis loop a fact that is conceived to need an explanantion.[2]

In the present communication, we address the first three points. We present results of a computer simulation on the adsorption in well-defined cylindrical pores. The experiments we wish to support by our model calculations have partly been carried out in Vycor[2,3] which is characterized by a highly connected pore network and in well-defined etched pores.[1] The relation between the behavior of single pores (domains) and networks of domains has been treated extensively in recent literature.[4,5] This is not in the focus of the present work, since important phenomena appear to be identical in connected and non-interconnected pores, e.g., the behavior in pressure jump experiments. Therefore, we content ourselves to modeling the adsorption in single cylindrical pores. The investigated system is a model system. In order to simulate a realistic situation, the

* To whom correspondence should be addressed. E-mail: hmorgner@rz.uni-leipzig.de.

10.1021/jp903717b
Published on Web 11/11/2009

parameters are chosen to describe the adsorption of argon in the mesoporous material SBA-15 at 77.35 K.[6]

Theory

The treatment of inhomogeneous systems in a thermodynamic framework requires some additional definitions, because classical thermodynamics is the only physical theory that does not know a distance coordinate. Thus, the theory is unable to formulate gradients which are characteristic for inhomogeneous systems. The two familiar strategies for this purpose are the square gradient method which has been introduced by Cahn and Hilliard[7] and reformulated recently by Bedeaux and coworkers[8] and the density functional method, e.g., refs 9 and 10. The approach which is employed in the present work is very akin to the density functional method. It has been developed during the past few years and applied to surface tension calculations, coalescence of nanodroplets, and the uptake of supercritical CO_2 into a water droplet.[11]

The general expression of the molar Helmholtz energy for a single component system is

$$A_{\mathrm{m}}(\rho, T) = U_{\mathrm{m}}(\rho, T) - TS_{\mathrm{m}}(\rho, T) \tag{1}$$

where ρ and T are the density of amount and the temperature, while and U_{m} and S_{m} denote molar internal energy and molar entropy. For an atomic compound, the internal energy can be split into the kinetic energy per mole and the molar potential energy due to interaction with surrounding particles

$$U_{\mathrm{m}}(\rho, T) = E_{\mathrm{kin,m}}(T) + E_{\mathrm{pot,m}}(\rho, T) \tag{2}$$

For isothermal processes the kinetic energy remains constant and, thus, can be omitted in describing the internal energy

$$U_{\mathrm{m}}(\rho, T) = E_{\mathrm{pot,m}}(\rho, T) \tag{3}$$

Now we will address the relation between the potential energy and the pair interaction potentials. As we wish to model the behavior of a fluid A in contact with a solid B we have to consider the following terms $E_{AA,pot}(\vec{r})$, $E_{AB,pot}(\vec{r})$, $E_{BB,pot}(\vec{r})$, $E_{BA,pot}(\vec{r})$, where $E_{X,Y,pot}(\vec{r})$ denotes the molar potential energy of species X at position $\vec{r}$ under the influence of species Y. The terms can be written as

$$E_{XY,\mathrm{pot}}(\vec{r}) = \int_{\mathrm{volume}} g_{XY}(|\vec{r} - \vec{r}'|)V_{XY}(|\vec{r} - \vec{r}'|)\rho_Y(\vec{r}')\,\mathrm{d}r'^3 \tag{4}$$

The functions in the integral are the density of amount $\rho_X(\vec{r})$ at the position $\vec{r}$, the interaction potential $V_{XY}(r)$ and the pair distribution function $g_{XY}(r)$ where $r = |\vec{r} - \vec{r}'|$. The latter two functions are conceived to depend only on the distance, but not on the direction. The suffixes X, Y denote the components A or B, respectivlely.

In a homogeneous environment one can take the densities of amount out of the integral to get position independent energies. If we further switch to spherical coordinates we can carry out the integration over the angles in closed form to obtain

$$E^{\mathrm{hom}}_{XY,\mathrm{pot}} = \rho_Y 4\pi \int_0^\infty g_{XY}(r)V_{XY}(r)r^2\,\mathrm{d}r \tag{5}$$

We define radial convolution functions via

$$f_{XY,r}(r) = \frac{g_{XY}(r)V_{XY}(r)}{E^{\mathrm{hom}}_{XY,\mathrm{pot}}\rho_Y^{-1}} \tag{6}$$

By this definition the radial convolution functions are normalized as

$$1 = 4\pi \int_0^\infty f_{XY,r}(r)r^2\,\mathrm{d}r$$

As $f_{AB,r}(r)$ and $f_{BA,r}(r)$ have the same shape and are both normalized, they must be identical.

$$f_{AB,r}(r) = f_{BA,r}(r)$$

This leads to the equality

$$\frac{E^{\mathrm{hom}}_{AB,\mathrm{pot}}(\rho_B)}{\rho_B} = \frac{E^{\mathrm{hom}}_{BA,\mathrm{pot}}(\rho_A)}{\rho_A}$$

and, thus, allows for the definition of the constant

$$-\theta_{AB}: = \frac{E^{\mathrm{hom}}_{AB,\mathrm{pot}}(\rho_B)}{\rho_B} = \frac{E^{\mathrm{hom}}_{BA,\mathrm{pot}}(\rho_A)}{\rho_A} \tag{7}$$

In the general case we have the expressions for the molar potential energy

$$E^{\mathrm{inh}}_{XY,\mathrm{pot}}(\vec{r}) = \int_V E^{\mathrm{hom}}_{XY,\mathrm{pot}}(\rho_Y(\vec{r}))\rho_Y^{-1}(\vec{r})f_{XY,r}(|\vec{r} - \vec{r}'|)\rho_Y(\vec{r}')\,\mathrm{d}r'^3 \tag{8}$$

As the first two factors of the integrand do not depend on the integration variable $\vec{r}'$ we can write

$$E^{\mathrm{inh}}_{XY,\mathrm{pot}}(\vec{r}) = \frac{E^{\mathrm{hom}}_{XY,\mathrm{pot}}(\rho_B(\vec{r}))}{\rho_Y(\vec{r})} \int_V f_{XY,r}(|\vec{r} - \vec{r}'|)\rho_Y(\vec{r}')\,\mathrm{d}r'^3 \tag{9}$$

With the definitions of convoluted densities of amount

$$\begin{aligned} \bar{\rho}_X(\vec{r}) &= \int_V f_{XX,r}(|\vec{r} - \vec{r}'|)\cdot\rho_X(\vec{r}')\,\mathrm{d}r'^3 \\ \bar{\rho}_{X,XY}(\vec{r}) &= \int_V f_{YX,r}(|\vec{r} - \vec{r}'|)\cdot\rho_X(\vec{r}')\,\mathrm{d}r'^3 \end{aligned} \tag{10}$$

we obtain

$$E^{\mathrm{inh}}_{AA,\mathrm{pot}}(\vec{r}) = \frac{E^{\mathrm{hom}}_{AA,\mathrm{pot}}(\rho_A(\vec{r}))}{\rho_A(\vec{r})}\bar{\rho}_A(\vec{r})$$
$$E^{\mathrm{inh}}_{BB,\mathrm{pot}}(\vec{r}) = \frac{E^{\mathrm{hom}}_{BB,pot}(\rho_B(\vec{r}))}{\rho_B(\vec{r})}\bar{\rho}_B(\vec{r})$$
$$E^{\mathrm{inh}}_{AB,\mathrm{pot}}(\vec{r}) = \frac{E^{\mathrm{hom}}_{AB,\mathrm{pot}}(\rho_B(\vec{r}))}{\rho_B(\vec{r})}\bar{\rho}_{B,AB}(\vec{r}) = -\theta_{AB}\bar{\rho}_{B,AB}(\vec{r})$$
$$E^{\mathrm{inh}}_{BA,\mathrm{pot}}(\vec{r}) = \frac{E^{\mathrm{hom}}_{BA,\mathrm{pot}}(\rho_A(\vec{r}))}{\rho_A(\vec{r})}\bar{\rho}_{A,AB}(\vec{r}) = -\theta_{AB}\bar{\rho}_{A,AB}(\vec{r}) \tag{11}$$

The total molar potential energy of the system due to internal interaction is then

$$E^{\mathrm{inh}}_{\mathrm{pot}}(\vec{r}) = x_A(E^{\mathrm{inh}}_{AA,\mathrm{pot}}(\vec{r}) + E^{\mathrm{inh}}_{AB,\mathrm{pot}}(\vec{r})) + x_B(E^{\mathrm{inh}}_{BB,\mathrm{pot}}(\vec{r}) + E^{\mathrm{inh}}_{BA,\mathrm{pot}}(\vec{r}))$$

With $\rho(\vec{r}) = \rho_A(\vec{r}) + \rho_B(\vec{r})$, $x_A = (\rho_A(\vec{r}))/(\rho(\vec{r}))$, and $x_B = (\rho_B(\vec{r}))/(\rho(\vec{r}))$, we get

$$E^{\mathrm{inh}}_{\mathrm{pot}}(\vec{r}) = \frac{E^{\mathrm{hom}}_{AA,\mathrm{pot}}(\rho_A(\vec{r}))}{\rho(\vec{r})}\bar{\rho}_A(\vec{r}) - \frac{\rho_A(\vec{r})}{\rho(\vec{r})}\theta_{AB}\bar{\rho}_{B,AB}(\vec{r}) + \frac{E^{\mathrm{hom}}_{BB,\mathrm{pot}}(\rho_B(\vec{r}))}{\rho(\vec{r})}\bar{\rho}_B(\vec{r}) - \frac{\rho_B(\vec{r})}{\rho(\vec{r})}\theta_{AB}\bar{\rho}_{A,AB}(\vec{r}) \tag{12}$$

For a fluid/fluid binary system all four terms have to be considered. However, the present paper is concerned with the interaction between a fluid and a solid. Microscopically, at any given location one has either the solid component B which leads to $\rho_A(\vec{r}) = 0$ or one has no solid which allows for $\rho_A(\vec{r}) > 0$ while $\rho_B(\vec{r}) = 0$. As a consequence, the density has to be written as

$$\rho(\vec{r}) = \begin{cases} \rho_A(\vec{r}) & \text{out side pore wall} \\ \rho_B(\vec{r}) & \text{wall of pore} \end{cases} \tag{13}$$

Outside the pore walls we get

$$E^{\mathrm{inh}}_{\mathrm{pot}}(\vec{r}) = \frac{E^{\mathrm{hom}}_{AA,\mathrm{pot}}(\rho_A(\vec{r}))}{\rho_A(\vec{r})}\bar{\rho}_A(\vec{r}) - \theta_{AB}\bar{\rho}_{B,AB}(\vec{r})$$

and inside the wall of the pores we have

$$E^{\mathrm{inh}}_{\mathrm{pot}}(\vec{r}) = \frac{E^{\mathrm{hom}}_{BB,\mathrm{pot}}(\rho_B(\vec{r}))}{\rho_B(\vec{r})}\bar{\rho}_B(\vec{r}) - \theta_{AB}\bar{\rho}_{A,AB}(\vec{r})$$

The solid wall of the pores is conceived to be rigid. The consequence is that the density $\rho_B(\vec{r})$ and the convoluted density $\bar{\rho}_B(\vec{r})$ do not change with time. Accordingly, the term $(\{E^{\mathrm{hom}}_{BB,\mathrm{pot}}[\rho_B(\vec{r})]\}/[\rho_B(\vec{r})])\bar{\rho}_B(\vec{r})$ remains constant during isothermal processes and, thus, can be neglected. The last term $\theta_{AB}\bar{\rho}_{A,AB}(\vec{r})$ measures the potential energy of the solid B under the influence of the fluid A. It has bearing onto the total energy balance and would have to be taken into account for the simulation of calorimetric measurements. Our interest, however, concerns isothermal processes which allow neglecting this term.

Inserting these results into eq 12 yields

$$E^{\mathrm{inh}}_{\mathrm{pot,m}}(\vec{r}) = \frac{E^{\mathrm{hom}}_{AA,\mathrm{pot}}(\rho_A(\vec{r}))}{\rho_A(\vec{r})}\bar{\rho}_A(\vec{r}) - \theta_{AB}\bar{\rho}_{B,AB}(\vec{r}) \tag{14}$$

The last term $\theta_{AB}\bar{\rho}_{B,AB}(\vec{r})$ plays the role of a position dependent external field acting on the fluid A. It does not depend on the shape of the density of amount of the fluid A.

The molar Helmholtz energy can then be written as

$$A_{\mathrm{m}}(\vec{r}) = \frac{E^{\mathrm{hom}}_{AA,\mathrm{pot}}(\rho_A(\vec{r}))}{\rho_A(\vec{r})}\bar{\rho}_A(\vec{r}) - \theta_{AB}\bar{\rho}_{B,AB}(\vec{r}) - TS_{\mathrm{m}}(\rho_A(\vec{r})) \tag{15}$$

This form of the Helmholtz energy is appropriate for isothermal situations of atomic compounds. The entropic term is not affected by inhomogeneity, as has been argued by Cahn and Hilliard[7] with reference to statistical mechanics.

In the planned simulation calculation the chemical potential will play a key role. The expression of the chemical potential shall fulfill the following requirements: it develops into the standard expression $\mu_A = A_{\mathrm{m}}(\rho_A) + \rho(\partial A_{\mathrm{m}}/\partial\rho_A(\rho_A))$ wherever the density ρ_A is constant; it takes on a constant value in the entire system at equilibrium, i.e., if the integral $\int_{\mathrm{volume}}\rho_A(\vec{r})A_{\mathrm{m}}(\rho_A(\vec{r}))\,\mathrm{d}r^3$ takes on a global minimum for constant amount $n_{\mathrm{A}} = \int_{\mathrm{volume}}\rho_A(\vec{r})\,\mathrm{d}r^3$ and constant volume.

The first condition is easily verified by equating the convoluted densities equal to the density and by removing the wall interaction by setting $\theta_{AB} = 0$.

The second condition is fulfilled by the following expression, as shown in the Supporting Information eq A.8

$$\mu_A(\vec{r}) = -TS_{\mathrm{m}}(\vec{r}) - \rho(\vec{r})T\left(\frac{\partial S_{\mathrm{m}}}{\partial\rho_A}(\vec{r})\right) + \left(\frac{\partial E^{\mathrm{hom}}_{AA,\mathrm{pot}}}{\partial\rho_A}(\rho_A(\vec{r}))\right)\bar{\rho}_A(\vec{r}) + \int_V \mathrm{d}^3r'\cdot(E^{\mathrm{hom}}_{AA,\mathrm{pot}}(\rho_A(\vec{r}'))\cdot f_{AA,r}(\vec{r}' - \vec{r})) - 2\theta_{AB}\bar{\rho}_{B,AB}(\vec{r}) \tag{16}$$

In the Supporting Information, the general case of a binary system is treated. The present system is special in that component B is solid and, thus, cannot relax into equilibrium. Only the fluid component A can be adjusted. We will employ the expression from eq A.8 as a working formula for determining the chemical potential of component A under the influence of the rigid component B. The shape of the density $\rho_A(\vec{r})$ is varied until the chemical potential $\mu_A(\vec{r})$ takes on a constant value throughout the system. Thus, the situation, which we establish by letting $\mu_A(\vec{r})$ take on a constant value, is not the global minimum of the Helmholtz energy which would be the case in a standard thermodynamical system. The above expression for the chemical potential is consistently valid for homogeneous and inhomogeneous systems. It is conceived to retain its meaning even in nonequilibrium.

With the above definition of the chemical potential we are in the position to treat diffusion for any given start situation via Onsager's ansatz[12] for constant temperature

$$\vec{J}_A = -\frac{L}{T}\,\mathrm{grad}\,\mu_A(\vec{r}) \tag{17}$$

rather than by Fick's law. This is an important aspect for a consistent treatment of gas phase adsorption in porous material. The condensation of vapor in porous material necessarily leads to a concentration in the pores that exceeds the concentration in the gas phase. As the driving force in Fick's law is the concentration gradient, it is obvious that filling of the pores via diffusion cannot be described by Fick's law without any additional assumptions. On the other hand, Onsager's ansatz explains the pore filling process against a concentration gradient in a consistent way. Usually, the coefficient L is not known. We evaluate this quantity from Fick's diffusion coefficient D as $L = \rho/R \cdot D$. It is worth noting that this does not affect the ability of Onsager's ansatz to describe diffusion against a concentration gradient.

At last we treat the pressure in the system. It is well-known that at inhomogeneities the definition of pressure becomes problematic. For treating planar interfaces it is common practice to introduce two different pressures P_N and P_T which are conceived as components of a pressure tensor.[13,14] The relation to the interface tension for a flat interface is given as

$$\sigma = \int_{-\infty}^{\infty} \mathrm{d}z(P_T(z) - P_N) \tag{18}$$

P_N can be identified with the pressure that is described by the EOS in the homogeneous regions on both sides of the interface. The pressure profile $P_T(z)$ which fulfills the above relation is shown in the Supporting Information (eq A.9) to be given as

$$P_T(z) = \rho_A(z)(\mu_A(z) - A_m(z)) + \rho_B(z)(\mu_B(z) - A_m(z))$$

With reference to eq 13 this reduces within the pores to

$$P_T(z) = \rho_A(z)(\mu_A(z) - A_m(z)) \tag{19}$$

or

$$P_T(\vec{r}) = \rho_A(\vec{r})(\mu_A(\vec{r}) - A_m(\vec{r}))$$

Via eqs 15 and 16 the pressure $P_T(\vec{r})$ is defined for all locations containing the fluid component A. For our purpose the relevance of eq 19 rests in the possibility that we can make use of surface tension data in order to determine the convolution function $f_{AA,r}(r)$. For this purpose it is useful to specify the convolution function for the case of a flat interface, i.e., for a situation that has gradients only in the direction z perpendicular to the flat interface. The 1-dimensional convolution function f_z and the radial convolution function f_r are related to each other by

$$f_z(z) = 2\pi \int_z^{\infty} f_r(r) r \, \mathrm{d}r$$

and

$$f(r) = -\frac{1}{2\pi}\left(\frac{\partial f}{\partial z}(z)\right)\frac{1}{z}\bigg|_{z=r} \tag{20}$$

The 1-dimensional convolution function f_z is normalized by definition as

$$1 = \int_{-\infty}^{\infty} f_z(z) \, \mathrm{d}z$$

Parametrization of the Model System

The goal of the present paper consists in clarifying by means of numerical calculations several aspects of adsorption in porous material from the gas phase. Even though we are not interested in describing one particular system, it appears reasonable to choose parameters that model a realistic system. We have chosen to select all parameters according to the experimental adsorption isotherm of argon to mesoporous silicate SBA-15 at $T = 77.35$ K.[6]

At first, we have to find an expression for the equation of state that describes fluid argon in the temperature range near and above 77 K reasonably well.[15] We have chosen a modified van der Waals equation of state

$$P = \frac{RT}{1/\rho_A - b} - a\rho_A^s$$

The three parameters employed are $a = 60694.3$ J·cm$^{3\cdot(s-1)}$/mol^s, $b = 23.63$ cm^3/mol, $s = 1.815$. The familiar relation $-(\partial A_m/\partial V_m)_T = P(\rho,T) = \rho^2(\partial A_m/\partial\rho)_T$ allows evaluating the molar Helmholtz energy as function of density ρ at constant temperature to be

$$A_m(\rho_A, T) = -RT \ln\left(\frac{1}{\rho_A} - b\right) - \frac{a}{s-1}\rho_A^{s-1} + C(T)$$

For isothermal applications the integration constant $C(T)$ can be omitted. If the coefficients a, b, s are treated as temperature independent, then the remaining two terms can be identified as the entropic term which leads to

$$S_m(\rho_A, T) = R \ln\left(\frac{1}{\rho_A} - b\right)$$

and the molar potential energy

$$E_{AA,pot}^{hom}(\rho_A, T) = -\frac{a}{s-1}\rho_A^{s-1}$$

Inserting this expression into eq 14 leads to

$$E_{pot,m}^{inh}(\vec{r}) = \frac{E_{AA,pot}^{hom}(\rho_A(\vec{r}))}{\rho_A(\vec{r})}\bar{\rho}_A(\vec{r}) - \theta_{AB}\bar{\rho}_{B,AB}(\vec{r}) = -\frac{a\cdot(\rho_A(\vec{r}))^{s-2}}{s-1}\bar{\rho}_A(\vec{r}) - \theta_{AB}\bar{\rho}_{B,AB}(\vec{r}) \tag{21}$$

As convolution function a simple Gaussian is chosen

$$f_r(r) = \left(\frac{a_{AA}}{\pi}\right)^{3/2}\exp(-a_{AA}\cdot r^2)$$

which has proven to combine simplicity with sufficient flexibility to model real components, e.g., the uptake of supercritical CO_2 into a water droplet.[11] The width of the Gaussian is determined by parameter a_{AA}. It is related to the half-maximum separation

via $r_{1/2} = \sqrt{(\ln(2)/a_{AA})}$. The corresponding 1-dimensional convolution function is

$$f_z(z) = \left(\frac{a_{AA}}{\pi}\right)^{1/2} \cdot \exp(-a_{AA} \cdot z^2)$$

Parameter a_{AA} is adjusted so as to reproduce via eqs 18, 19, 21 the surface tension of argon at $T = 90.67$ K ($\sigma = 11.65$ mN/m).[16] The parameters collected so far allow simulating the argonlike component at low temperature including the gas/condensed interface. A distinction between solid and liquid argon is not made. As the triple point is expected to drop in pores to smaller values of temperature and pressure,[17] the condensed argon in pores is assumed to be a supercooled liquid. Experimental evidence supports this notion. Only well below 70 K has freezing of argon been observed in mesopores.[1]

Now, we have to model the interaction between the fluid and the solid that constitutes the porous material. As we do not wish to simulate caloric experiments it is sufficient to describe the effect of the solid material onto the adsorbed component, expressed by the second term of eq 14

$$\theta_{AB}\bar{\rho}_{B,AB}(\vec{r}) = \theta_{AB} \int_V f_{AB,r}(|\vec{r} - \vec{r}'|)\rho_B(\vec{r}')\, \mathrm{d}r'^3$$

If we assume the density of amount within the solid wall to be constant, we can take ρ_B outside the integral and carry out the integral over the volume of the solid

$$\theta_{AB}\bar{\rho}_{B,AB}(\vec{r}) = \theta_{AB}\rho_B \int_{\text{volumeofsolid}} f_{AB,r}(|\vec{r} - \vec{r}'|)\, \mathrm{d}r'^3$$

Accordingly, we have to determine the constant $\theta_{AB}\rho_B$ and the convolution function $f_{AB,r}(r)$. Again we choose a Gaussian for the convolution function

$$f_{AB}(r) = \left(\frac{a_{AB}}{\pi}\right)^{3/2} \cdot \exp(-a_{AB} \cdot r^2)$$

which depends only on the range of the interaction as measured by parameter a_{AB}.

The two constants $\theta_{AB}\rho_B$ and a_{AB} are adjusted to reproduce the experimental adsorption isotherm of argon to mesoporous silicate SBA-15 at $T = 77.35$ K[6] at low relative pressure P/P_0. At low pressure the pore structure has negligible influence on the isotherm. Thus, the two parameters $\theta_{AB} \cdot \rho_B$ and a_{AB} describe the interaction between adsorbate and solid wall without reference to the curvature of the wall. The parameters are available in the following table.

quantity	value	units
a_{AA}	5.162	nm^{-2}
$\theta_{AB}\rho_B$	10215.95	J/mol
a_{AB}	6.912	nm^{-2}

Comparing the parameters a_{AA} and a_{AB} indicates that the interaction within the fluid is of longer range than the interaction between fluid and solid material.

The influence of the curvature of the pore wall shows up in the evaluation of the convoluted densities of amount $\bar{\rho}_A(\vec{r})$ and $\bar{\rho}_{B,AB}(\vec{r})$, cf. eqs 10 and 15. The scheme of the pore geometry is shown in Figure 1. We have made use of the cylindrical symmetry of the pores which reduces the numerical effort somewhat. As mentioned above, the quantity $\bar{\rho}_{B,AB}(\vec{r})$ depends only on the pore geometry and thus remains unchanged during the calculation of an isotherm. On the other hand, the convoluted density of the fluid $\bar{\rho}_A(\vec{r})$ has to be evaluated for any new distribution of the fluid within the simulated volume. The calculation is carried out with the spatial step width set to $\Delta z = \Delta r = 0.126$ nm. This leads to about 10 000 points within the simulated volume.

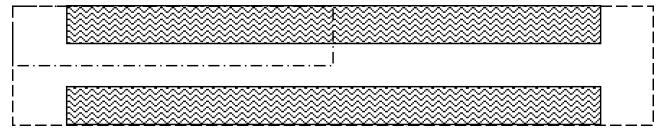

Figure 1. Scheme of the simulated pores. The dashed line defines the simulated volume. The pore material is shaded, the pore radius being constant. The pore is in contact with the gas phase at both ends. The density of the gas phase is kept constant at left and right borders of the simulated volume. The length of the pores is 62 nm. The diameter varies between 4.8 and 6.6 nm. The computational effort is reduced by making use of symmetry properties. The calculation is carried out in cylindrical coordinates with no explicit angular dependence of the fluid density. This leads to a 2-dimensional calculation. Further, the fluid density is assumed to be symmetric with respect to the mirror plane in the middle of the pore. Thus, only the upper left part of the pore is calculated.

Results and Discussion

With the chemical potential of the adsorbate set up as described above, it is possible to model any desired pore structure and study its influence on the adsorption isotherm at any pressure. Calculations are restricted to $P/P_0 < 1$, but it is worthwhile to note that $P/P_0 > 1$, i.e., adsorption out of the liquid phase would not require any additional effort.

We have carried out simulations for a cylindrical pore which is in physical contact with the gas phase on both ends. The isotherm is determined by setting the density of the gas phase outside the pore at a separation from the pore mouth which is equal to the pore radius. The gas pressure outside the pore is changed stepwise, and thus, the nominal chemical potential for the entire system. The system is then allowed to exchange adsorbate between gas phase and pore as long as the chemical potential anywhere in the system deviates from the nominal value. Only if the chemical potential within the entire system deviates by less than $\Delta\mu = 10^{-4}$ J/mol from the nominal value will the simulation stop. The total amount of adsorbate within the pore is evaluated and divided by the inner surface of the pore wall. Thus, the amount of adsorbed fluid is obtained in units of mol/cm^2 for any given outside vapor pressure. The resulting isotherm is not affected if the threshold value $\Delta\mu$ is increased by a factor of 10. The calculations have been carried out for six pore diameters in the range 4.8−6.6 nm in order to simulate a realistic pore size distribution. It is shown as an insert in the plot of the isotherm, see Figure 2. All quantities shown in the figures represent weighted averages over the pore size distribution. The isotherm in Figure 2 displays a hysteresis loop which is very similar to the experimental data from ref 6.

The diffusion coefficient is constructed in the following way. The viscosity of the model fluid as function of density is taken to be that of argon.[18] The diffusion coefficient $D(\rho)$ as function of density is evaluated via the Stokes−Einstein relation, with the atomic radius of argon set to 0.198 nm. The simulation of pressure jump experiments is calculated with the position dependent quantity $D(\rho(\vec{r}))$, with the diffusion coefficient depending on the position only via the local density $\rho(\vec{r})$.

The data in Figure 3 refer to the evaluation of the mean self-diffusion coefficient in equilibrium. For lack of better input data,

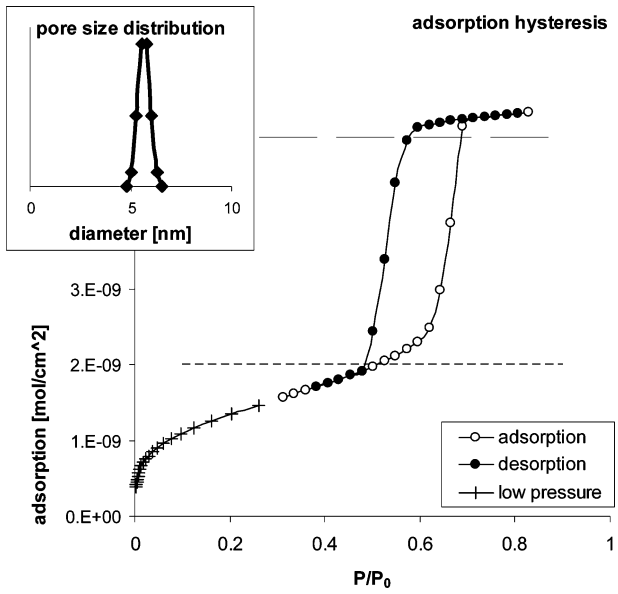

Figure 2. Simulated isotherm in mesoporous material. The pore size distribution is shown in the insert. The parameters in the simulation are chosen to model the system Argon/SBA-15 at 77.35 K.

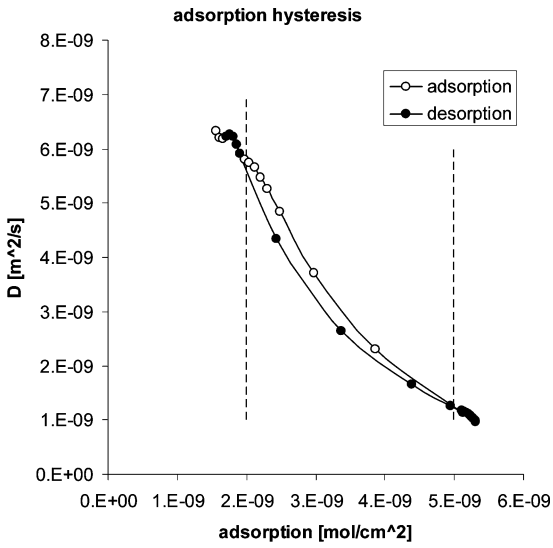

Figure 3. Self-diffusion coefficient, evaluated as weighted average in the pores.

I have equated the self-diffusion coefficient with the dynamic diffusion coefficient. It is then straightforward to derive the mean self-diffusion coefficient via

$$D_{\text{mean}} = \frac{\int_{\text{porevolume}} D(\rho(\vec{r}))\cdot\rho(\vec{r})\,\mathrm{d}r^3}{\int_{\text{porevolume}} \rho(\vec{r})\,\mathrm{d}r^3}$$

The result is shown in Figure 3. Within the hysteresis loop, the self-diffusion coefficient D_{mean} appears to be larger during adsorption compared to desorption, for the same amount of pore filling. Thus, the characteristic features observed in the experiment[2] are reproduced well. The replacement of the self-diffusion coefficient by the dynamic diffusion coefficient can be justified by assuming that both coefficients are monotonous functions of the density in the relevant range of densities between 0.00002 and 0.038 mol/cm^3. If so, the qualitative observation that the averaged self-diffusion deviates between adsorption and desorption branch is not affected.

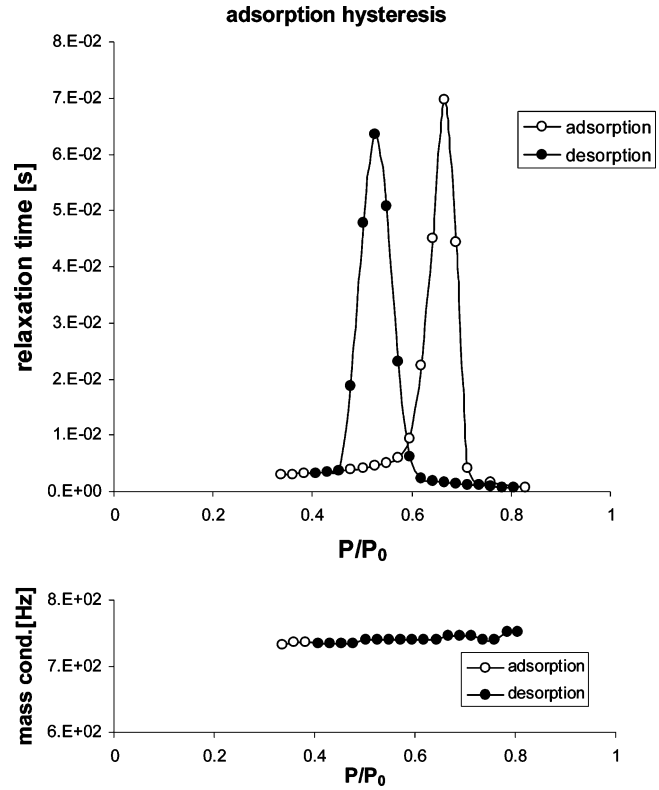

Figure 4. Upper panel shows relaxation time τ as function of the reduced pressure. Lower panel shows mass conductivity $\sigma = (\mathrm{d}f/\mathrm{d}p)\cdot\tau^{-1}$ as defined in ref 1.

Further, we have simulated pressure jump experiments. For this purpose the density distribution in the pore is propagated in time via eq 17. The relaxation time has been evaluated from the time dependence of the adsorption given in units of [mol/cm^2], by fitting an exponential function. Again, good agreement is found with experimental findings. The relaxation time varies by ca. 2 orders of magnitude as is the case in the experiment,[1] cf. Figure 4. The mass conductivity, defined as the ratio between the slope of the isotherm and the relaxation time in ref 1, is evaluated as well and shown in the lower panel of Figure 4. Wallacher et al.[1] have proposed an approximate proportionality between the measured relaxation time and the slope of the isotherm. Their notion is fully supported by the present simulation. The proportionality factor varies only mildly in the entire pressure range; in particular, it goes smoothly through the hysteresis region.

An explanation of this behavior can be given in simple terms: the pressure change ΔP is the same for both cases, namely for the pressure being varied outside the hysteresis or inside the hysteresis. Thus, the driving force is similar while the amount of fluid to be transferred from the gas reservoir into the pore system is very different, depending on the slope of the isotherm. Outside the hysteresis, the slope is smaller than that near the switching points of the hysteresis. If the same diffusional transport mechanism is active in both cases, one would expect that relaxation into the equilibrium state takes longer inside the hysteresis loop where the slope is larger than outside the hysteresis, as has actually been observed.

In Figure 5, the reaction of the system during incomplete passage through the hysteresis loop is shown. The related diffusion coefficient is displayed in Figure 6. One observes that the key features found experimentally are found as well in the simulation: when we evaluate the averaged diffusion coefficients along the scanning curves we find that the diffusivities are located within the range established by the complete hysteresis

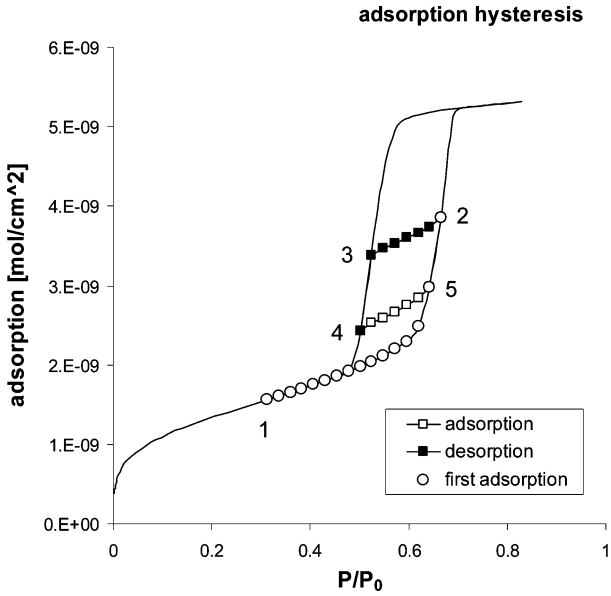

Figure 5. Adsorption behavior for incomplete passage through the hysteresis loop. Adsorption starts at point 1 at a pressure below capillary condensation and is followed up to point 2, i.e., before the completion of the hysteresis loop. Then, the pressure is lowered via point 3 to point 4 and stopped again within the hysteresis loop. Increase of pressure leads back to point 2 via point 5. This incomplete loop can be followed repeatedly. Further explanation continues in the text.

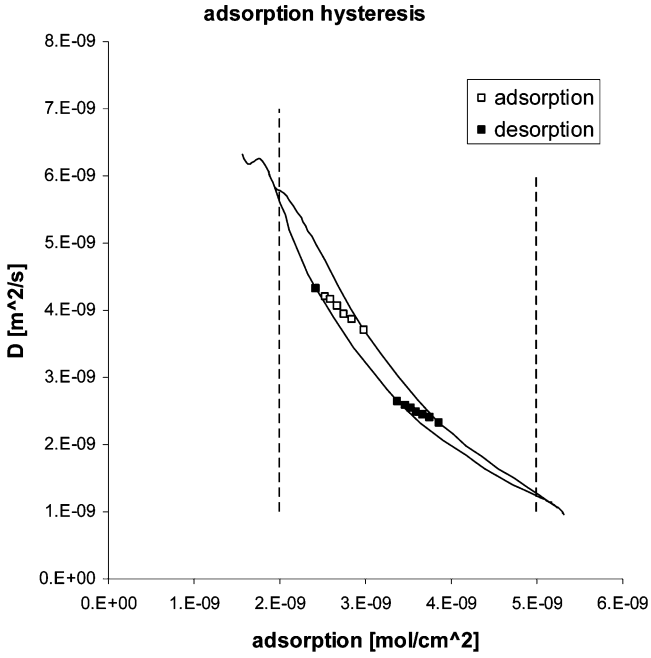

Figure 6. Diffusion coefficient during incomplete passage through the hysteresis loop, evaluated as weighted average in the pores. The full line represents the values from Figure 3.

loop, in agreement with the experiment.[3] This observation does not require any additional concept as suggested by S. Naumov et al.[3] They discuss a memory effect caused by avoided equilibration due to high free energy barriers.

The observed phenomenon is easily explained by the fact that we deal with a system that is composed of pores with different pore diameters. The following observations can be made by inspecting the results of the simulation in detail. Any pore diameter has two well-defined switching points (switching pressure or switching chemical potential). If one stops the adsorption before the apparent hysteresis loop is completed, then this means that the pores with smaller diameter have switched into the high load state while the pores with larger diameter have not. Lowering the pressure in the consecutive desorption cycle follows the desorption branch of the isotherm for the small diameter pores, but leaves the large diameter pores in the adsorption branch of the isotherm. No explanation beyond the mere existence of hysteresis is needed.

Conclusion and Outlook

The present work demonstrates that all experimental features observed so far for adsorption of fluids in mesopores can be accounted for on the basis of standard physical concepts. The results suggest to avoid statements which imply to postulate new transport mechanisms ("a fundamental difference in the nature of the relaxation dynamics for states within the hysteresis region") or postulation of "activated state dynamics" in the pore. We concede, though, that the mere fact that all phenomena can be calculated in the simulation does not yet give a satisfying answer as to the nature of the states or to the mechanisms involved. In a forthcoming publication we will address the nature of the states within the hysteresis loop in a rigorous thermodynamic concept.

Acknowledgment. The theoretical basis of this study has been developed with financial support by the German Science Foundation under Grant Mo288/26 within the Priority program 1105 "Non equilibrium processes in Fluid/fluid systems". The author acknowledges stimulating discussions with W. Janke, R. Gläser, and J. Kärger.

Note Added after ASAP Publication. This article was published ASAP on November 11, 2009. Equation 17 has been revised. The correct version was published on April 22, 2010.

Supporting Information Available: Additional details and equations. This material is available free of charge via the Internet at http://pubs.acs.org.

References and Notes

(1) Wallacher, D.; Künzer, N.; Kovalev, D.; Knorr, N.; Knorr, K. *Phys. Rev. Lett.* **2004**, *92*, 195704–1.
(2) Valiullin, R.; Naumov, S.; Galvosas, P.; Kärger, J.; Woo, H.-J.; Porcheron, F.; Monson, P. *Nature* **2006**, *443*, 965–968.
(3) Naumov, S.; Valiullin, R.; Monson, P. A.; Kärger, J. *Langmuir* **2008**, *24*, 6429–32.
(4) Coasne, B.; Gubbins, K. E.; Pellenq, R. J.-M. *Phys. Rev. B* **2005**, *72*, 024304.
(5) Grosman, A.; Ortega, C. *Langmuir* **2008**, *24*, 3977–86.
(6) Rockmann, R. Ph.D. Thesis, University Leipzig, 2007.
(7) Cahn, J. W.; Hilliard, J. E. *J. Chem. Phys.* **1958**, *28*, 258–267.
(8) Bedeaux, D.; Johanessen, E.; Rosjorde, A. *Physica* **2003**, *A330*, 329–5. Johanessen, E.; Bedeaux, D. *Physica* **2003**, *A330*, 354.
(9) Tarazona, P.; Evans, R. *Mol. Phys.* **1984**, *52*, 847–57.
(10) Wadewitz, T.; Winkelmann, J. *Phys. Chem. Chem. Phys.* **1999**, *1*, 3335–43.
(11) Morgner, H. Final Report, Priority Program 1105 of the Deutsche Forschungsgemeinschaft "Nonequilibrium Processes in Fluid/Fluid Systems", 2007.
(12) Göpel, W.; Wiemhöfer, H.-D. *Statistische Thermodynamik*; Spektrum, Akademischer Verlag: Heidelberg, 2000.
(13) Walton, J. P. R. B.; Tildesley, D. J.; Rowlinson, J. S. *Mol. Phys.* **1983**, *48*, 1357–68.
(14) Allen, M. P. *Chem. Phys. Lett* **2000**, *331*, 513–8.
(15) van Witzenburg, W. *Phys. Lett. A* **1967**, *25*, 293–4.
(16) Sprow, F. B.; Prausnitz, J. M. *Trans. Faraday Soc.* **1966**, *62*, 1105–11. Sprow, F. B.; Prausnitz, J. M. *Trans. Faraday Soc.* **1966**, *62*, 1097–104.
(17) Thommes, M. *Nanoporous Materials: Science and Engeneering*; Lu, G. Q., Zhao, X. S., Eds.; Imperial College Press: London, 2004.
(18) *CRC Handbook of Chemistry and Physics*; Lide, D. R., Ed.; CRC Press: New York, 1999.

JP903717B